Field Measurement Results of the 15 T Nb3Sn Dipole Demonstrator

J. DiMarco, M. Baldini, E. Barzi, V.V. Kashikhin, I. Novitski, T. Strauss, M. Tartaglia, G. V. Velev, A.V. Zlobin

***Abstract*— A 15 T Nb3Sn dipole with cos-theta-type coils was developed to demonstrate a possible magnet design for a post-LHC proton-proton Collider. The magnet has 4-layer coils with 60-mm aperture, and has graded current density between the inner and outer layers to maximize performance. The coils are constrained by vertically-split, thick iron laminations, connected by aluminum I-clamps, and a thick stainless-steel skin. The magnet was previously tested at the Vertical Magnet Test Facility (VMTF) at Fermilab with reduced pre-load, and achieved record 14.1 T fields at maximum current. Now the magnet has been reassembled with full pre-load and has been cryogenically retested at VMTF. We report here on the magnetic measurements results of these tests, including field strength, geometrical harmonics, coil magnetization, and iron saturation characteristics of the demonstrator.**

***Index Terms*—Superconducting magnets, Electromagnetic measurements, Accelerator magnets**

I. Introduction

FERMILAB, in collaboration with members of the US Magnet Development Program (US-MDP), has fabricated a 15 T Nb3Sn dipole demonstrator suitable for a post-LHC hadron collider [1]. The magnet, MDPCT1, was based on an optimized "cos-theta" coil design and was tested in 2019 [1-3]. This same magnet, having been reassembled with additional shims to bring it to full preload as compared to its original build, and now designated MDPCT1b, has been recently tested at Fermilab's Vertical Magnet Test Facility. In this new configuration, the test focused on study of magnet quench performance and changes in field quality.

The MDPCT1 design has 60 mm aperture and 4-layer shell-type graded coils. Details of magnet design, fabrication and performance in the original build have been reported previously [1]. The details of MDPCT1b re-assembly and quench performance, are reported in another paper to this conference [4].

Here we present the results of the MDPCT1b magnetic measurements, including dipole strength, geometrical field harmonics, and magnetization and yoke saturation effects, emphasizing field changes with respect to the original build [5]. Moreover, results from measurements of sextupole decay during simulated injection porch studies are also presented.

This work is supported by Fermi Research Alliance, LLC, under contract No. DE-AC02-07CH11359 with the U.S. Department of Energy, Office of Science, Office of High Energy Physics.

The authors are with Fermi National Accelerator Laboratory, P.O. Box 500, Batavia, IL 60510, USA, (e-mail: dimarco@fnal.gov).

II. Field Definition and Measurement System

The measured field of a dipole is expressed in a standard form of harmonic coefficients defined in a series expansion of a complex field function

$$B_y + iB_x = B_1 10^{-4} \sum_{n=1}^{\infty} (b_n + ia_n) \left(\frac{x+iy}{R_{ref}}\right)^{n-1} \qquad (1)$$

where B_x and B_y in (1) are the field components in Cartesian coordinates, b_n and a_n are the normal and skew coefficients at reference radius R_{ref}, normalized to the main field, B_1, and scaled by a factor 10^4 so as to report the harmonics in convenient 'units'. In the presented analysis, for better comparison, all measurements utilize R_{ref}, of 17 mm, which is the nominal value for the LHC dipole magnets. The right-handed measurement coordinate system is defined with the z-axis at the center of the magnet aperture and pointing from return to lead end, with z=0 at magnet center.

The rotating coil technique is used to measure field components. The two measurement probes are built on circuit board technology [6] and have a 13 turn PCB pattern with a maximum turn length of 26 mm x 10 mm wide (22.7 mm integrated length, "26 mm probe") and 130 mm x 10 mm wide (126.8 mm integrated length, "130 mm probe") respectively. The latter probe length approximately corresponds to one transposition/twist pitch of the cable. Each probe has a dipole bucked signal to increase measurement accuracy of harmonics. The probe radius of 14 mm was constrained by the anti-cryostat diameter used for measurement. It is about 20% less than the reference radius R_{ref}.

The integration component of the data acquisition system is based on ADC and digital signal processor technology [7]. The system can digitize simultaneously up to 6 channels measuring the magnetic field plus the current signal, tolerating a high rotational probe speed. To mitigate the noise from the mechanical vibrations and to record the voltages from the strong dipole field, we used a probe speed of 0.67Hz. At this speed, the combined probe and DAQ sensitivity was estimated to be about 0.1 units for a_n and b_n harmonics up to n=7.

Currents for the magnetic measurements were limited to 9kA to limit the possibility of additional quenches.

III. Measurement Results and Discussion

A. Magnet Transfer Function

Figure 1 shows the measured Transfer Function (TF) (where TF=B_1/I) of MDPCT1b versus the magnet current overlayed with the original MDPCT1 result. As for the TF measurement

in the original magnet, we use the 26mm probe to calculate magnet strength at high field [5]. The slight differences in TF at low and high fields between MDPCT1b and MDPCT1 are interesting and may suggest slightly different saturation. With the close TF overlay, calculation of field strength from current at quench should be the same as for MDPCT1, within the 0.2% difference observed.

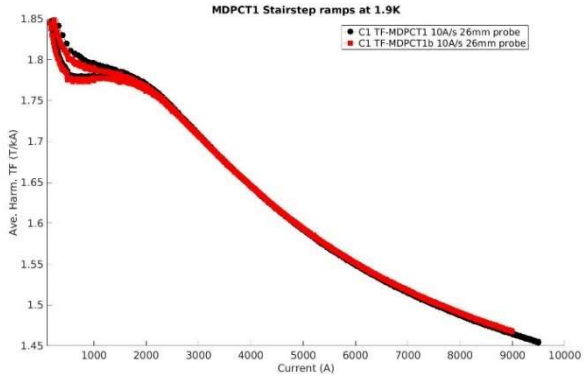

Fig. 1. Measured dipole TF versus current for MDPCT1b compared to MDPCT1 with the 26mm probe. A small negative offset is seen for 1b at low fields and a small positive difference at high field.

Figure 2 shows axial variation of *TF* at 9 kA, measured using short and long rotating coil probes. The non-lead 'half' is slightly stronger by about 15-20 units, again perhaps stemming from smaller saturation effects. The average TF across the magnet, therefore, is ~0.1% higher in MDPCT1b than in the original build. Note that only a few unit increase is expected from coil compression from added shims, so this difference may be related to a difference in gap closure of the two halves between builds. As noted in [5], the small increase of the transfer function in the ends is predicted by the 3D COMSOL simulation [8].

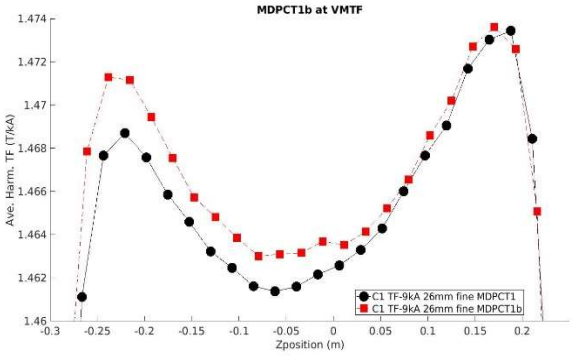

Fig. 2. Measured dipole TF at 9kA versus magnet Z-position for MDPCT1b compared to MDPCT1 with the 26mm probe. The 1b TF is larger for the non-lead end half, but is about the same at the lead end.

B. *Low-order field harmonics*

Figure 3 shows axial variation of the low order normal (b_2, b_3, b_4 and b_5) and skew (a_2, a_3, a_4 and a_5) harmonics. The harmonics are generally small (being less than ±5 units in the magnet straight section (±0.3 m)), except for b_3, and have not changed much with the rebuild, except for a_3, which shows a 2-3 units shift, and for some differences at the lead end of the skew harmonics, presumably because of the shims.

A comparison of the harmonics dependence on current for the two builds is shown in Figure 4. Again, there is generally very good consistency, with no large changes caused by the added shims except for a_3, which shows the largest change in hysteresis character, and b_3 and a_2, which also show some shift. Perhaps coil asymmetry, which likely generates discrepancy between dipole and sextupole field directions, has gotten slightly worse after the shimming.

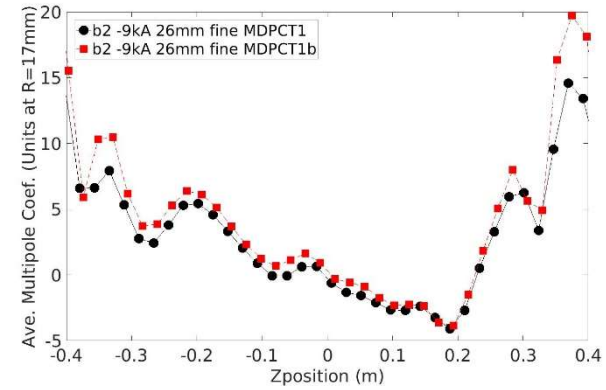

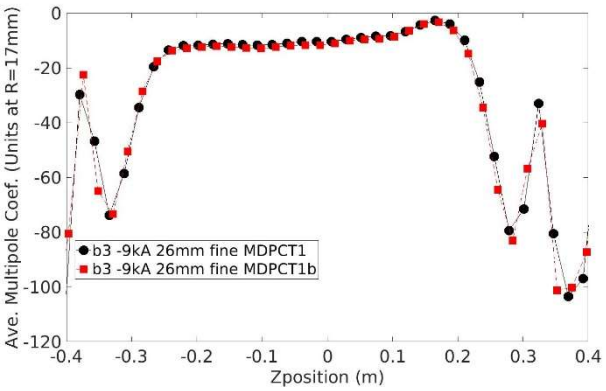

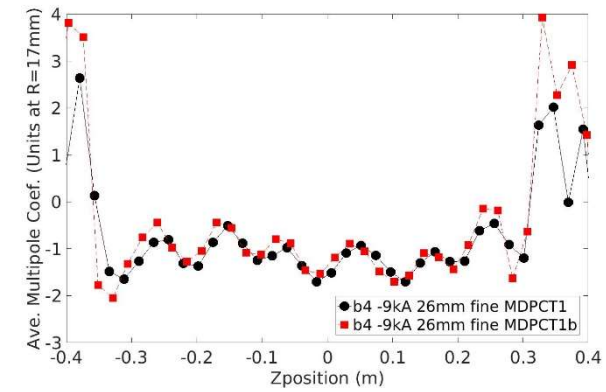

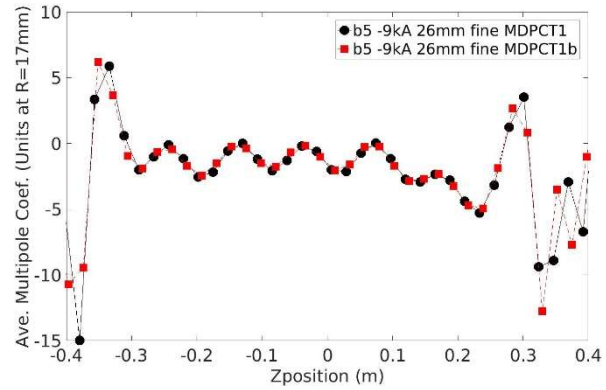

Fig. 3a. Low-order normal (b_n) coefficients vs Z at 9kA for MDPCT1 (black) and MDPCT1b (red).

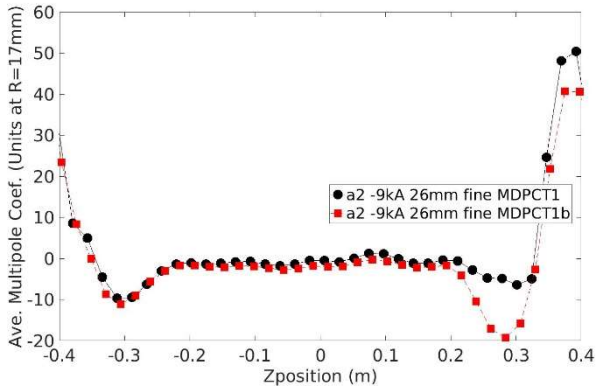

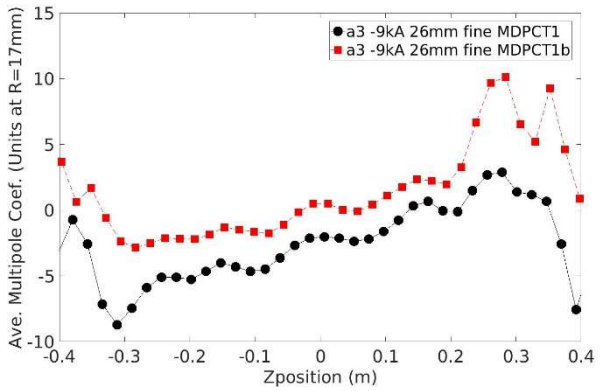

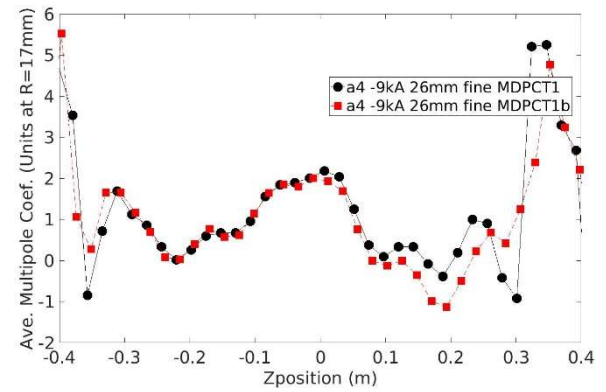

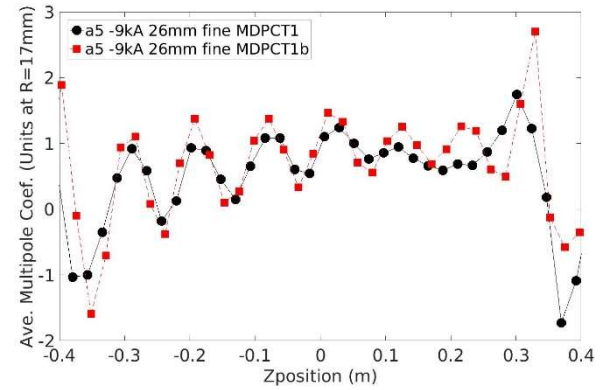

Fig. 3b. Low-order skew (a_n) coefficients vs Z at 9kA for MDPCT1 (black) and MDPCT1b (red).

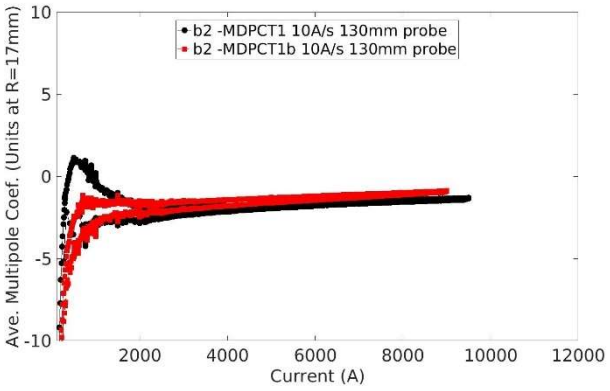

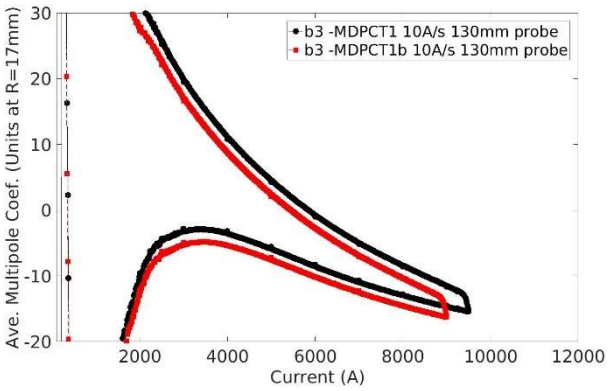

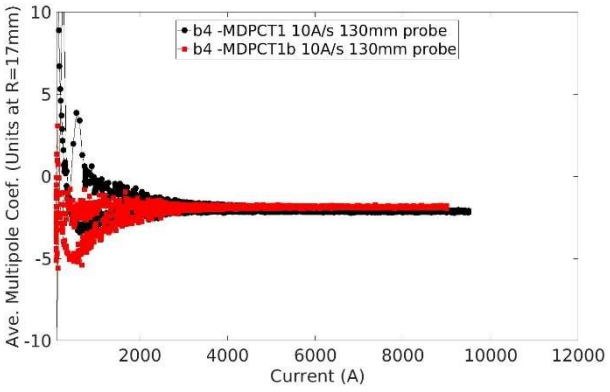

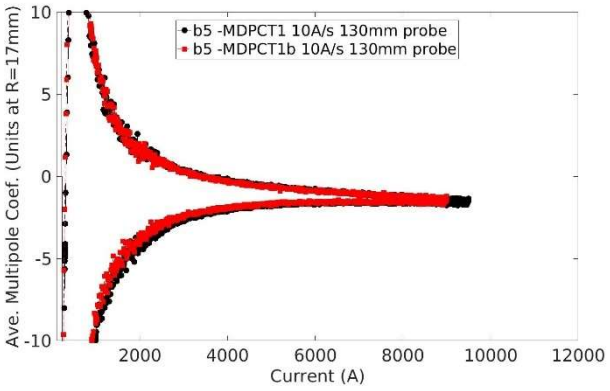

Fig. 4a. Low-order normal (b_n) coefficients vs I at 9kA for MDPCT1 (black) and MDPCT1b (red).

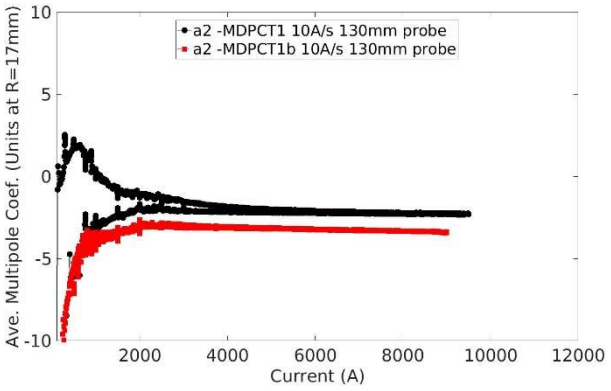

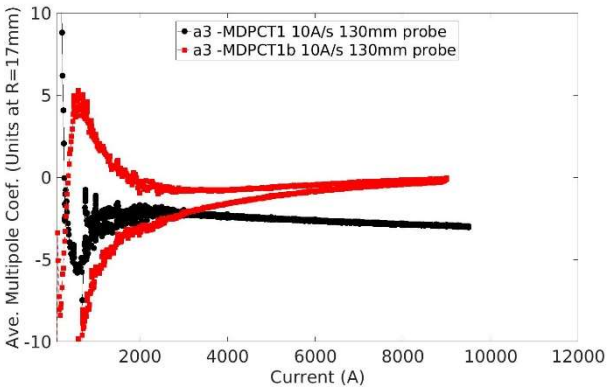

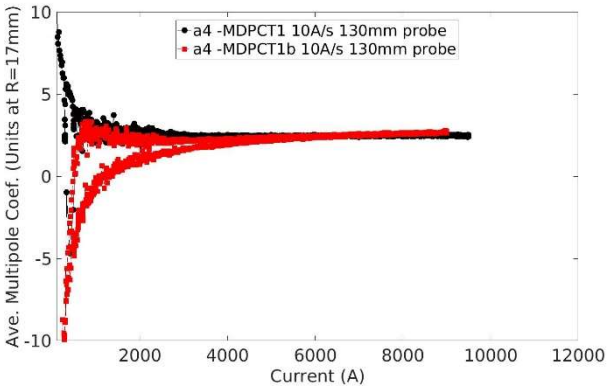

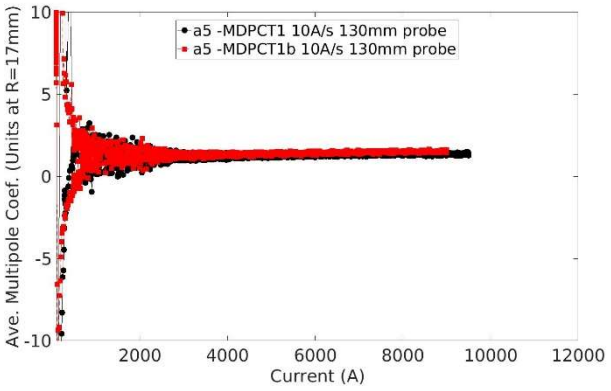

Fig. 4b. Low-order skew (a_n) coefficients vs I at 9kA for MDPCT1 (black) and MDPCT1b (red).

C. *Snapback and decay*

To make a further study of decay and snapback at a simulated injection current, measurements were made during the current cycle shown in Figure 5, with data taken by both with 130mm and 26mm probes, which sample at different z-positions (the centers separated by 130mm). Before this current profile, a pre-cycle ramps the magnet to 9000A and holds for 5 minutes before returning to a holding current of 100A to achieve a reproducible magnetization state. The harmonics decay is measured for 30 minutes upon reaching the simulated injection porch at 1100A, and continues through snapback as upramp current ramping resumes. Similar measurements are made on the 'back porch' as the current ramps down after its cycle to 9000 A. After this first cycle, when the current is back at 100 A, the probe positions are shifted by 6 cm downward (half a cable transposition pitch), and the simulated injection cycle repeated.

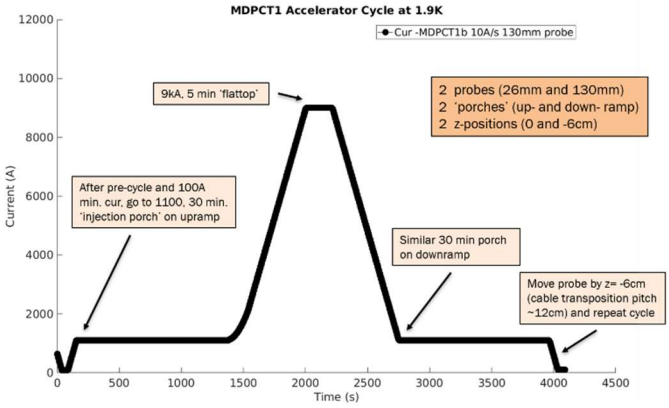

Fig. 5. Current profile used for harmonic decay and snapback measurements during accelerator cycle simulation.

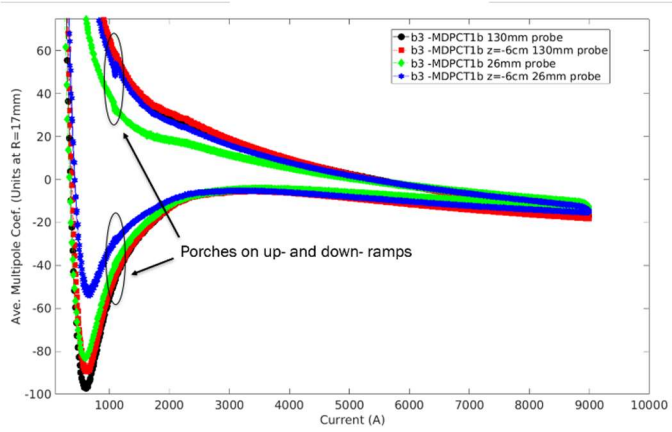

Fig. 6. b_3 hysteresis with injection 'porches' during accelerator profile.

The normal sextupole hysteresis cycle during the accelerator profile is shown in Figure 6. Results of the decay and snapback measurements are shown in Figures 7 and 8 for the up-ramp and down-ramp porches respectively. Note that data have been offset for clarity as noted in the legends. The 130mm probe data seems to be fairly stable with regards to the -6cm shift in Z-

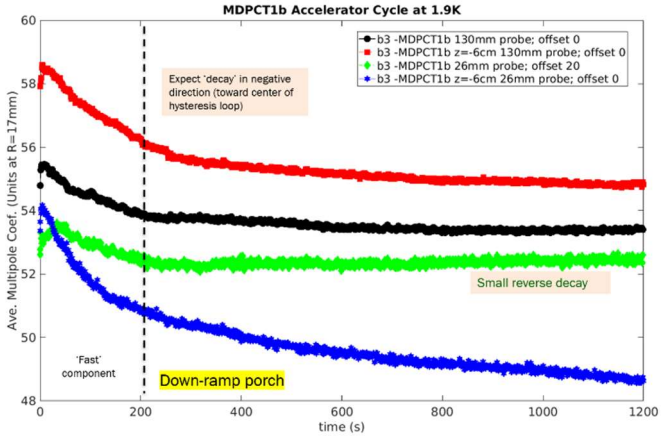

Fig. 7. b_3 decay and snapback on the 'front' porch during up-ramp to 1100A.

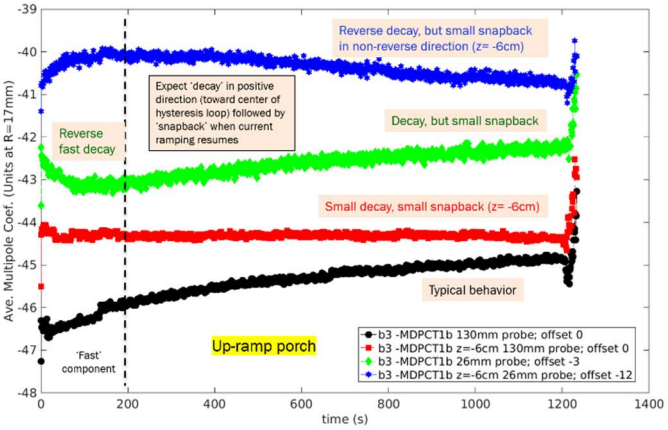

Fig. 8. b_3 decay and snapback on 'back' porch during down-ramp to 1100A

position. The up-ramp decay becomes more flat, indicating some dependence on position (or perhaps the effect of the small mismatch between 11 cm cable transposition pitch and the 13 cm probe length), while the down-ramp decay seems very similar.

The 26cm probe, which should be much more sensitive to the transposition pitch, shows more interesting changes. First, the decay is reversed between porches on the up-ramp and down-ramp for both initial and shifted positions, and then these all reverse at some level when the probe position is changed. This sensitivity seems to suggest that the decay is related to the Boundary Induced Coupling Currents (BICC) that also create periodicity in some of the harmonics wrt Z-position [9] – evident, for example, in b_4, b_5 and a_5 in Figure 3.

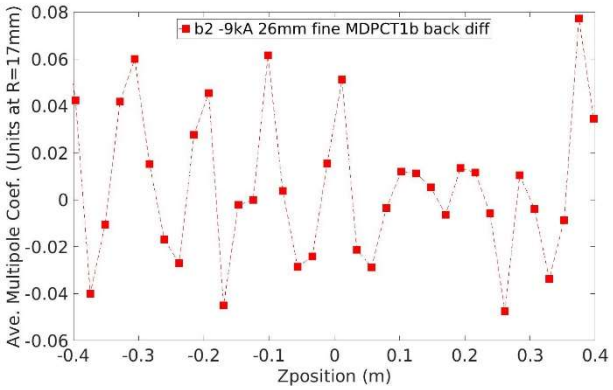

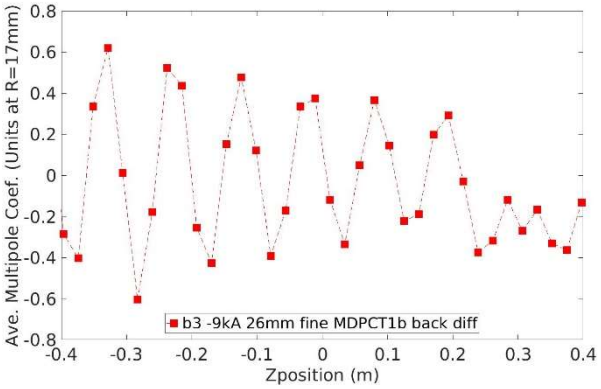

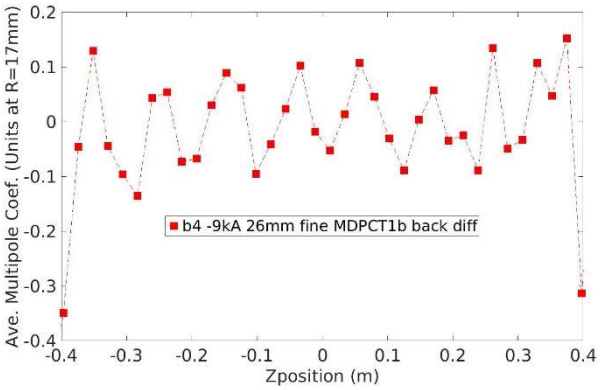

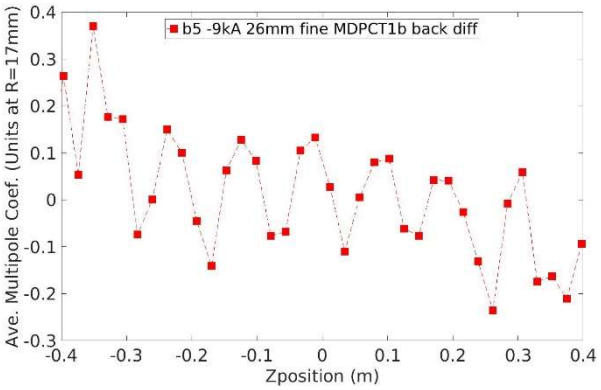

Fig. 9a. Difference in b_n harmonics between scan taken in the forward Z-direction, followed by a scan taken moving in the reverse Z-direction.

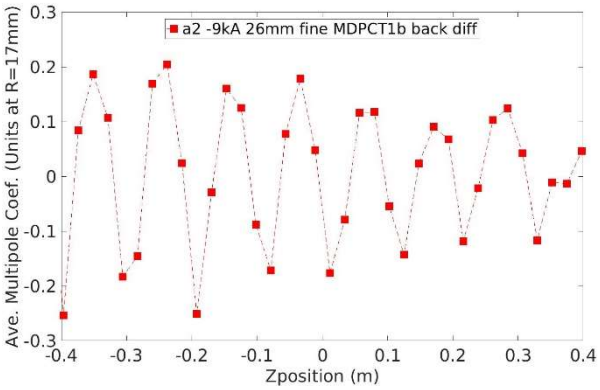

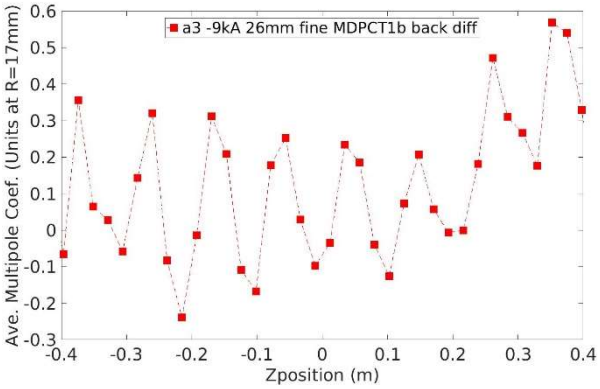

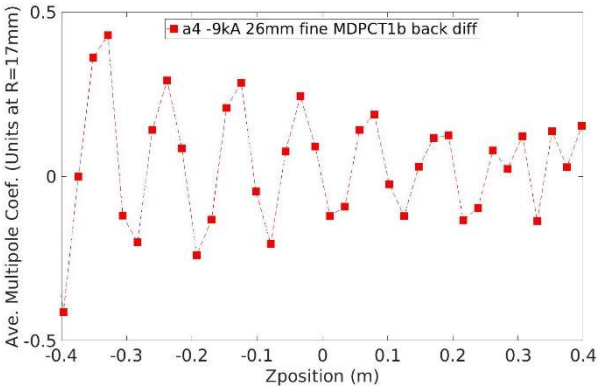

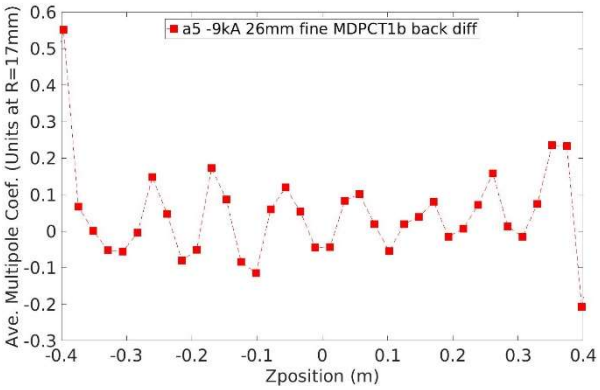

Fig. 9b. Difference in a_n harmonics between scan taken in the forward Z-direction, followed by a scan taken moving in the reverse Z-direction.

To further look at the decay of the BICC, axial scans were performed in a forward direction (from -0.6m to +0.6m), followed by scans taken moving in the reverse direction axially, i.e. from +0.6m to -0.6m at 9kA. The results of the difference between forward and reverse scans are shown in Figure 9. Clear periodic patterns are present in all the harmonics, demonstrating that the periodicity is related not only to transposition pitch, but also to change in time: presumably as the BICC decay in the intervening delay between Z-scan samples at a given point. The measurements were repeated at 5kA, and similar effects seen, but with a reduced amplitude.

IV. CONCLUSION

The dipole field strength and field harmonics for the rebuilt 15 T dipole demonstrator MDPCT1b recently tested at Fermilab have been presented. The average transfer function has increased by ~0.1% from changes in the non-lead half of the magnet. Harmonics are basically the same except for some small changes in normal and skew sextupole and other small changes at the lead end. Some harmonics (b_2, a_4) also show change between lead-end and non-lead-end halves similar to that seen in the TF. We hope to learn more about the causes of some of the subtle changes in harmonics during the disassembly inspection.

In the study of decay and snapback of sextupole, we find that local variations in measurement position with a non-transposition-pitch-integral (short) probe can cause substantially different decay profiles. We also observe that the periodic pattern associated with twist pitch changes in time (between forward and reverse z-scans in our measurements), suggesting, therefore, that both the local variation and change in time effects are related to current re-distribution in the cable.

ACKNOWLEDGMENT

The authors would like to thank the technical staff of Fermilab's Applied Physics and Superconducting Technology Division for their contribution to the magnet testing.

REFERENCES

[1] A. V. Zlobin *et al*., "Development and First Test of the 15 T Nb3Sn Dipole Demonstrator MDPCT1," in *IEEE Transactions on Applied Superconductivity*, vol. 30, no. 4, pp. 1-5, June 2020, Art no. 4000805, doi: 10.1109/TASC.2020.2967686.

[2] A.V. Zlobin et al., "Design concept and parameters of a 15 T Nb3Sn dipole demonstrator for a 100 TeV hadron collider", Proceedings of IPAC2015, Richmond, VA, USA, p.3365.

[3] I. Novitski et al., "Development of a 15 T Nb3Sn Accelerator Dipole Demonstrator at Fermilab", IEEE Trans. on Appl. Supercond., Vol. 26, Issue 3, June 2016, 4001007.

[4] A. V. Zlobin et. Al, "Reassembly and Test of High-Field Nb3Sn Dipole Demonstrator MDPCT1", in proceedings of this conference.

[5] T. Strauss et al., "First Field Measurements of the 15 T Nb3Sn Dipole Demonstrator MDPCT1," in IEEE Transactions on Applied Superconductivity, vol. 30, no. 4, pp. 1-6, June 2020, Art no. 4001106, doi: 10.1109/TASC.2020.2970621.

[6] J. DiMarco et al., "Application of PCB and FDM Technologies to Magnetic Measurement Probe System Development", IEEE Trans. on Appl. Supercond., Vol. 23, Issue 3, 2013, p. 9000505.

[7] G.V. Velev et al., "A Fast Continuous Magnetic Field Measurement System Based on Digital Signal Processors", IEEE Trans. of Applied Superconductivity, Vol. 16, No. 2, June 2006, pp. 1374-1377.

[8] COMSOL Multiphysics, https://www.comsol.com.

[9] G. Velev, et al., "Summary of the Persistent Current Effect Measurements in Nb3Sn and NbTi Accelerator Magnets at Fermilab", IEEE Trans. Appl. Supercond., Vol. 26, No. 4, 2016, Art. 4000605.